Mediating Molecular Recognition by Methionine Oxidation: Conformational Switching by Oxidation of Methionine in the Carboxyl-Terminal Domain of Calmodulin †

ARTICLE *in* BIOCHEMISTRY · AUGUST 2005

Impact Factor: 3.02 · DOI: 10.1021/bi0504963 · Source: PubMed

Mediating Molecular Recognition by Methionine Oxidation: Conformational Switching by Oxidation of Methionine in the Carboxyl-Terminal Domain of Calmodulin†

Asokan Anbanandam,‡,§ Ramona J. Bieber Urbauer,|| Ryan K. Bartlett,‡,⊥ Heather S. Smallwood,# Thomas C. Squier,# and Jeffrey L. Urbauer*,||,@

Department of Chemistry, University of Georgia, Athens, Georgia 30602, Department of Biochemistry and Molecular Biology, University of Georgia, Athens, Georgia 30602, Department of Molecular Biosciences, University of Kansas, Lawrence, Kansas 66045, and Cell Biology and Biochemistry Group, Biological Sciences Division, Fundamental Sciences Directorate, Pacific Northwest National Laboratory, P.O. Box 999, Richland, Washington 99352

Received March 17, 2005; Revised Manuscript Received May 18, 2005

ABSTRACT: The C-terminus of calmodulin (CaM) functions as a sensor of oxidative stress, with oxidation of methionine 144 and 145 inducing a nonproductive association of the oxidized CaM with the plasma membrane Ca^{2+}-ATPase (PMCA) and other target proteins to downregulate cellular metabolism. To better understand the structural underpinnings and mechanism of this switch, we have engineered a CaM mutant (CaM-L7) that permits the site-specific oxidation of M144 and M145, and we have used NMR spectroscopy to identify structural changes in CaM and CaM-L7 and changes in the interactions between CaM-L7 and the CaM-binding sequence of the PMCA (C28W) due to methionine oxidation. In CaM and CaM-L7, methionine oxidation results in nominal secondary structural changes, but chemical shift changes and line broadening in NMR spectra indicate significant tertiary structural changes. For CaM-L7 bound to C28W, main chain and side chain chemical shift perturbations indicate that oxidation of M144 and M145 leads to large tertiary structural changes in the C-terminal hydrophobic pocket involving residues that comprise the interface with C28W. Smaller changes in the N-terminal domain also involving residues that interact with C28W are observed, as are changes in the central linker region. At the C-terminal helix, $^{1}H^{\alpha}$, $^{13}C^{\alpha}$, and ^{13}CO chemical shift changes indicate decreased helical character, with a complete loss of helicity for M144 and M145. Using ^{13}C-filtered, ^{13}C-edited NMR experiments, dramatic changes in intermolecular contacts between residues in the C-terminal domain of CaM-L7 and C28W accompany oxidation of M144 and M145, with an essentially complete loss of contacts between C28W and M144 and M145. We propose that the inability of CaM to fully activate the PMCA after methionine oxidation originates in a reduced helical propensity for M144 and M145, and results primarily from a global rearrangement of the tertiary structure of the C-terminal globular domain that substantially alters the interaction of this domain with the PMCA.

The versatile calcium signaling protein calmodulin (CaM)[1] binds to an imposing array of cellular targets and modulates their functions (*1*). Target recognition is realized by hydrophobic clefts in each of the two globular domains of CaM that flank the central linker region. Of the solvent accessible hydrophobic surface area in these sites, an impressive and unusual 46% is contributed by methionine residues (*2*). This exposure renders these methionine residues susceptible to oxidation, and both in vivo and in vitro, all nine are known to undergo oxidation readily to the corresponding sulfoxides (*3*−*5*).

It has been known for some time that CaM is functionally sensitive to oxidation of its methionine residues (*6*−*8*). More recently, extensive functional characterization of the interac-

† This work was supported by the NIH (Grant AG17996), an instrument grant from the NSF (DBI 0088931), the University of Kansas, and the Office of the Vice President for Research at the University of Georgia. A.A. was supported by an American Heart Association Postdoctoral Fellowship (0120666Z).

* To whom correspondence should be addressed: Department of Biochemistry and Molecular Biology, University of Georgia, 120 Green St., Davison Life Sciences Complex, Athens, GA 30602-7229. Phone: (706) 542-7922. Fax: (706) 542-1738. E-mail: urbauer@chem.uga.edu.

‡ University of Kansas.

§ Present address: Department of Biochemistry and Molecular Biology, University of Texas-Houston Medical School, Houston, TX 77030.

|| Department of Biochemistry and Molecular Biology, University of Georgia.

⊥ Present address: Molecular Physiology and Biophysics, Vanderbilt University Medical Center, 724 Robinson Research Building, Nashville, TN 37232.

Pacific Northwest National Laboratory.

@ Department of Chemistry, University of Georgia.

[1] Abbreviations: C28W, peptide corresponding to the calmodulin-binding domain of the plasma membrane Ca^{2+}-ATPase; CaM, calmodulin; CaM_{ox}, calmodulin with all nine methionine residues oxidized to the sulfoxides; CaM-L7, calmodulin mutant with all methionine residues except M144 and M145 mutated to leucine; $CaM\text{-}L7_{ox}$, CaM-L7 with both M144 and M145 oxidized to the sulfoxides; CSI, chemical shift index; HSQC, heteronuclear single-quantum correlation; NMR, nuclear magnetic resonance; PMCA, plasma membrane Ca^{2+}-ATPase/calcium pump.

10.1021/bi0504963 CCC: $30.25
Published on Web 06/18/2005

tion of oxidized CaM (CaM_{ox}) with the plasma membrane Ca^{2+}-ATPase (PMCA) has been ongoing. The results have shown that CaM_{ox} is able to bind to the PMCA but not fully activate it (*3*−*5*, *9*−*12*). Whereas binding of CaM shifts the equilibrium between (auto)inhibited and active forms far toward the active form, binding of CaM_{ox} shifts the equilibrium only partially toward the active form, resulting in a partial nonproductive interaction (*3*−*5*, *9*−*12*). Not all of the methionine residues, when oxidized, contribute to the observed nonproductive interaction, and the earlier data indicated that only oxidation of the vicinal pair at the carboxyl-terminal end of CaM (M144 and M145) was necessary (*3*, *5*, *9*). More recent studies confirmed the role of M144 and M145 using CaM mutants that permitted site-selective methionine oxidation (*10*).

Some of the consequences of methionine oxidation in CaM for both CaM structure and target activation have been elucidated. Methionine oxidation decreases substantially the Ca^{2+} binding affinity of CaM (*3*, *13*), suggesting important structural changes modulating Ca^{2+} binding. Fluorescence and circular dichroism measurements have suggested a higher degree of dynamic disorder in the CaM binding domain of the PMCA when it is bound to oxidized CaM, suggesting that oxidized CaM does not induce the structural transitions that are essential for activation (*9*). Structural changes in the N-terminal globular domain of CaM have been suggested following oxidation of methionine residues in the C-terminal globular domain, as has a loss of conformational coupling between the N- and C-terminal domains involving the central linker region (*4*). The sensitivity to oxidation of particular methionine residues in CaM has also been correlated with the time-averaged surface accessibility of the sulfur atoms (*5*).

Herein, we present an examination of the structural implications of methionine oxidation for CaM and for a mutant CaM (CaM-L7) bound to the CaM-binding region of the PMCA (a 28-residue peptide, denoted C28W). The CaM-L7 mutant, in which all of the methionine residues except M144 and M145 have been replaced with leucine, permits the effects of oxidation of M144 and M145 to be selectively studied. We have demonstrated this approach to be tenable, as even substitution of all nine methionine residues in CaM with leucine does not alter its ability to activate the PMCA and does not radically perturb its structure (*10*). We have used NMR spectroscopy to monitor the spectral changes and measure both the main chain and side chain chemical shift changes that occur when M144 and M145 are oxidized to define and localize the structural changes that result. Accordingly, we have assigned the chemical shifts for the main chain and nearly all of the side chain nuclei for the CaM-L7 portions of both the CaM-L7−C28W complex and this complex with M144 and M145 oxidized to the corresponding sulfoxides, allowing these assessments. In addition, NMR experiments for selectively observing intermolecular contacts between CaM-L7 and the C28W peptide were performed to ascertain how oxidation of M144 and M145 in this complex alters the CaM−PMCA interface. Our results indicate that there is little secondary structural perturbation associated with methionine oxidation in CaM, with the exception of the C-terminal helix, and that oxidation of M144 and M145 causes a substantial, global perturbation of the C-terminal globular domain tertiary structure. Most notably, many of the important contacts between hydrophobic side chain groups in the C-terminal globular domain of CaM-L7 and C28W are lost upon oxidation of M144 and M145. We propose that the C-terminal domain reorganization and resulting inability to form the proper sequence-specific contacts with the PMCA CaM binding sequence thwart the proper structural stabilization or induction in this sequence which is obligatory for PMCA activation.

EXPERIMENTAL PROCEDURES

Calmodulin Preparation. Recombinant vertebrate calmodulin [from the chicken gene, accession number MCCH (PIR database) or P02593 (SWISS-PROT database)] and CaM-L7 (CaM with all methionine residues except M144 and M145 replaced with leucine) were produced as described previously (*10*). Isotopic labeling was accomplished by growing the bacteria [*Escherichia coli* BL21(DE3), Novagen, Madison, WI] harboring the CaM expression plasmid (pET-15b, Novagen) on minimal medium (M9) using uniformly ^{13}C-labeled glucose and uniformly ^{15}N-labeled ammonium chloride (Isotec Inc., Miamisburg, OH) as the sole carbon and nitrogen sources, respectively. The mutagenesis which produces the CaM-L7 mutant has been described previously (*10*). CaM and CaM-L7 were purified by hydrophobic interaction chromatography using Phenyl-Sepharose CL-4B (Pharmacia, Piscataway, NJ) essentially as described previously (*14*). The concentration of CaM was determined spectrophotometrically using the published extinction coefficient (*14*, *15*).

Oxidation of Calmodulin. The methionine residues in CaM and mutant CaM species were oxidized using H_2O_2 with H_2O_2 removal by exhaustive dialysis upon completion of the reaction (*10*). Reactions were performed at 25 °C for 24 h in the presence of excess (10 mM) $CaCl_2$. Oxidation was complete as judged by electrospray ionization mass spectrometry (*10*, *12*).

CaM−*C28W Complexes for NMR*. A 28-residue peptide (LRRGQILWFRGLNRIQTQIRVVNAFRSS) corresponding to the calmodulin binding domain of the plasma membrane Ca^{2+}-ATPase (PMCA), denoted C28W, was synthesized and purified commercially (BioSource International, Hopkinton, MA). The purity was confirmed by analytical reversed-phase HPLC, and the mass was confirmed (3385.8 Da vs a theoretical value of 3385.9 Da) by electrospray ionization (ESI) mass spectrometry using a Q-Tof quadrupole time-of-flight hybrid instrument (Micromass Ltd., Manchester, U.K.). The amino acid sequence of the peptide was also confirmed by tandem mass spectrometry. The complexes of C28W with CaM-L7 and oxidized CaM-L7 ($CaM\text{-}L7_{ox}$) were prepared by titration of the CaM species with the peptide under dilute conditions on ice. The samples were concentrated using Centricon YM3 ultrafiltration units (Millipore, Bedford, MA). The final concentrations of components in samples for NMR (700 μL) were approximately 1 mM protein or peptide, 50 mM KCl, 10 mM $CaCl_2$, 5 mM imidazole-d_4, 0.02% NaN_3, and 10% D_2O at pH 6.5.

Circular Dichroism Spectroscopy. The circular dichroism (CD) spectra were acquired at 25 °C using a Jasco 710/810 spectrapolarimeter. Samples contained 20 μM CaM species, 5 mM $CaCl_2$, 5 mM KCl, and 5 mM MES (pH 6.5). Data

points were collected from 190 to 250 nm using a 0.1 cm cuvette. Secondary structure calculations from the circular dichroism data were performed using a variety of algorithms available via the DichroWeb site (*16*−*18*). The best results were normally obtained using the CDSSTR algorithm (*19*−*22*), and are reported.

NMR Spectroscopy. All NMR spectra were recorded at 25 °C using Varian INOVA 600 MHz spectrometers equipped with triple-resonance pulse field gradient probes. The ^{1}H chemical shifts were referenced with respect to external Na^+DSS^- in D_2O (0.0 ppm) at 25 °C. The ^{15}N and ^{13}C chemical shifts were referenced indirectly assuming the following absolute frequency ratios: $^{15}N/^1H = 0.101\,329\,118$ and $^{13}C/^1H = 0.251\,449\,530$ (*23*). All data were processed and analyzed with Felix (Accelrys, San Diego, CA).

For both the CaM-L7−C28W complex and the CaM-L7$_{ox}$−C28W complex, the main chain and most of the side chain resonances have been assigned for the CaM components of the complexes. The main chain assignment strategy followed a normal triple-resonance approach employing uniformly ^{15}N- and ^{13}C-labeled CaM-L7 or CaM-L7$_{ox}$ bound to the unlabeled C28W peptide. Two-dimensional ^{1}H−^{15}N and ^{1}H−^{13}C HSQC and three-dimensional HNCA, HN(CO)CA, HNCACB, CBCA(CO)NH, HNCO, and HBHA(CBCACO)NH spectra were recorded for the sequential assignment of the main chain (^{1}HN, ^{15}N, $^1H^\alpha$, $^{13}C^\alpha$, ^{13}CO, and $^{13}C^\beta$). Side chain resonances were assigned using three-dimensional amide-resolved TOCSY and HCCH-TOCSY spectra. Assignment of aromatic side chains was assisted using two-dimensional (Hβ)Cβ(CδCγ)Hδ (*24*) and three-dimensional TOCSY-HMQC (*25*) spectra. Stereospecific assignment of the methyl groups of valine and leucine residues was accomplished using a CaM-L7$_{ox}$−C28W complex with the CaM portion 10% ^{13}C-labeled (*26*). In complexes with the C28W peptide, intermolecular NOEs between isotopically labeled CaM-L7 or CaM-L7$_{ox}$ and the unlabeled C28W peptide were selectively observed using a three-dimensional ^{13}C F_1-filtered, F_3-edited NOESY-HSQC experiment (*27*).

RESULTS

Retention of Secondary Structure in CaM upon Methionine Oxidation. The quantitative and selective oxidation of all nine methionine residues in CaM (Ca^{2+}_4-CaM) to the corresponding sulfoxides (CaM$_{ox}$) can be accomplished in vitro using H_2O_2 as the oxidant; no other amino acids are modified (*3*, *10*, *28*). Oxidation results in a mixture of (*R*)- and (*S*)-methionine sulfoxide isomers at the individual sites (*29*, *30*). Oxidation of all methionine residues results in little overall change in secondary structure of calcium-loaded vertebrate CaM (Ca^{2+}_4-CaM) as judged by the far-UV circular dichroism spectra (Figure 1A). A decrease in α-helical content from ∼59 to ∼55% is estimated on the basis of the CDSSTR algorithm (*19*−*22*). This small decrease in helical content is consistent with that reported for wheat germ calmodulin (*4*, *9*) but is somewhat smaller than the 11% loss of α-helical content reported upon complete oxidation of a hybrid calmodulin molecule [hybrid of mammalian and plant CaM (*13*)]. Results of previous studies with vertebrate CaM have, however, suggested large decreases in the α-helical content accompanying oxidation at low Ca^{2+} concentrations or higher temperatures (*31*, *32*). With the hybrid CaM molecule,

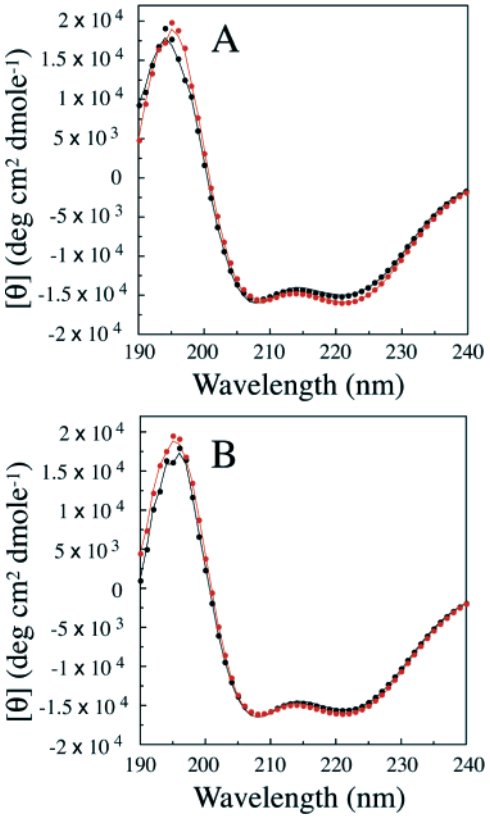

FIGURE 1: Secondary structure changes accompanying methionine oxidation in CaM and CaM-L7. Circular dichroism spectra before (red) and after (black) methionine oxidation for wild-type CaM (A) and CaM-L7 (B). Symbols represent experimental data, and lines represent the fits of the data as described in the text. In all cases, oxidations were performed and the spectra acquired in the presence of a saturating (10 mM) $CaCl_2$ concentration at 25 °C (see the text).

conditions that include low Ca^{2+} concentration have also been shown to result in dramatic changes in secondary structure (*13*). When complete oxidation is performed in the presence of high Ca^{2+} concentrations (10 mM in our experiments) at 25 °C, the secondary structure of the oxidized CaM is not perturbed substantially.

Oxidation-Induced Change in CaM Tertiary Structure. Changes in the tertiary structure of CaM upon methionine oxidation are apparent from a consideration of the chemical shift changes in the NMR spectra of CaM that accompany oxidation. The ^{1}H−^{15}N HSQC NMR spectrum of CaM$_{ox}$ (Ca^{2+}_4-CaM$_{ox}$) reveals a pattern of peaks similar to that observed in the corresponding CaM spectrum (Figure 2A). Most of the signature cross-peaks that define the important elements of the tertiary structure of CaM are still observed, indicating that the protein is still folded and the two globular domains remain intact and nativelike. However, oxidation perturbs the chemical shifts of most of the cross-peaks in the spectrum and also causes an increased conformational heterogeneity, reflected in the somewhat larger line widths. Thus, oxidation has clearly caused significant changes in the tertiary structure of CaM. The mixture of CaM$_{ox}$ species resulting from both (*R*)- and (*S*)-methionine sulfoxides at each site (*29*, *30*) also contributes to the conformational heterogeneity and increased line widths. Oxidation-induced tertiary structural changes could also lead to an increased level of aggregation, consistent with the increased line widths. The structural changes are likely to underlie the

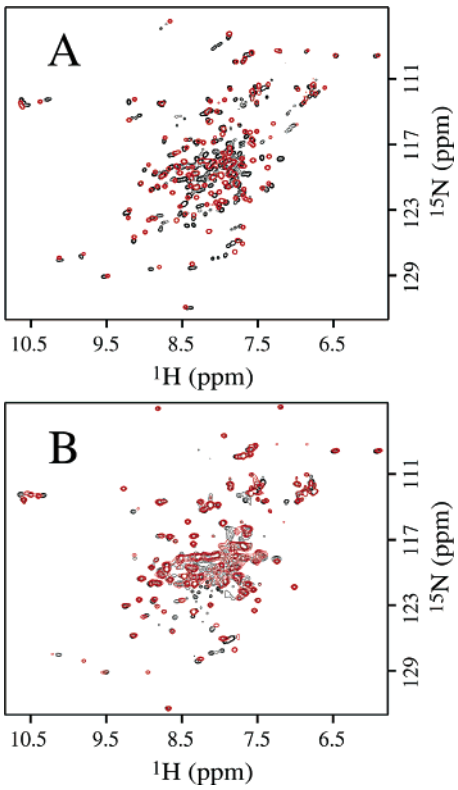

FIGURE 2: Effect of methionine oxidation on CaM and CaM-L7 structure. Two-dimensional $^{1}H-^{15}N$ HSQC spectra of CaM (A) and CaM-L7 (B) before (red contours) and after (black contours) oxidation of all methionine residues to the sulfoxides are shown. The spectra before and after oxidation were acquired on samples with equal concentrations under identical conditions (see the text) and are drawn at similar contour levels. Only positive contours are drawn.

observed changes in function, in particular, the weakened ability of CaM_{ox} to promote dissociation of the PMCA autoinhibitory domain relative to CaM (*3*−*5*, *9*−*12*).

Structural Changes in CaM-L7 upon Methionine Oxidation. The results of previous studies have suggested that oxidation of one or more C-terminal methionine residues (M144 or M145) in CaM is responsible for the inability of CaM_{ox} to fully activate the plasma membrane calcium ATPase (PMCA) (*3*, *5*). Recently, we have confirmed these suggestions using CaM mutants (leucine replacing methionine) that permit site-selective oxidation of these methionine residues (*10*). Functionally, methionine-to-leucine mutations in CaM have little effect on the ability of the mutant CaM to maximally activate the PMCA. In fact, the maximal stimulation of the PMCA by CaM-L7 (CaM with seven methionine residues mutated to leucine, leaving only M144 and M145) is larger than that by wild-type CaM (*10*). Moreover, the same is true for CaM-L9 (CaM with all nine methionine residues replaced with leucine). Thus, functionally, leucine substitution has served well as a method for allowing site-specific methionine oxidation.

Structurally, as judged by $^{1}H-^{15}N$ HSQC NMR spectra, we have previously shown that CaM-L9 (Ca^{2+}_{4}-CaM-L9) retains the tertiary structural features that define the calmodulin molecule, consistent with the functional results (*10*). The dispersion and chemical shifts of the cross-peaks indicate that the protein is still folded and the two globular domains remain intact and nativelike. Not surprisingly, therefore, the overall fold of CaM-L7 is also very similar to that of wild-type CaM (Figures 1B and 2B). As with wild-type CaM, oxidation of M144 and M145 in CaM-L7 results in little change in secondary structure. The circular dichroism spectra of CaM-L7 and CaM-$L7_{ox}$ (Figure 1B) indicate clearly, as expected from the results with CaM, that oxidation of M144 and M145 in CaM-L7 does not alter the secondary structure of CaM-L7 appreciably. There is no apparent change in the α-helical content upon oxidation (∼61 vs ∼62%). However, as with CaM, oxidation of CaM-L7 (CaM-$L7_{ox}$) does induce moderate changes in tertiary structure as indicated by the chemical shift changes observed throughout the $^{1}H-^{15}N$ HSQC spectrum of CaM-$L7_{ox}$ compared to that of CaM-L7 (Figure 2B). Increased line widths are also observed, suggesting a limited, increased conformational heterogeneity. Thus, these results indicate that the structural changes that accompany oxidation of methionine residues in CaM and promote the nonproductive interaction of CaM with the PMCA result primarily from tertiary structural changes that occur when M144 and M145 are oxidized. The results also illustrate the utility of the CaM-L7 mutant in the selective identification of the structural changes accompanying M144 and M145 oxidation, which is crucial for characterizing the structural basis for the nonproductive association of oxidized CaM with the PMCA.

Binding of C28W to CaM-L7 and CaM-$L7_{ox}$. The association of CaM with the CaM-binding sequence of the PMCA activates the PMCA by inducing dissociation of the autoinhibitory domain. Oxidation of M144 and M145 in CaM interferes with the activation process. Presumably, CaM induces critical structural changes in the CaM binding sequence essential for activation that are not induced when M144 and M145 are oxidized. To understand the process of PMCA activation by CaM and why oxidation of M144 and M145 thwarts the activation process, we have used NMR to measure structural differences in complexes of CaM-L7 and CaM-$L7_{ox}$ with a peptide corresponding to the CaM-binding sequence of the PMCA (C28W).

CaM binds with high affinity to C28W, and oxidation only marginally reduces its affinity (*12*). The dissociation constants for the CaM−C28W complex (no oxidation) have been measured to be 0.6 ± 0.2 and 4 ± 1 μM for the C- and N-terminal globular domains of CaM, respectively, whereas for the complex with oxidized CaM (from senescent rat brains, heterogeneously oxidized), these values are 0.4 ± 0.2 and 16 ± 8 μM, respectively (*12*). Functional studies with fully oxidized CaM and CaM-L7 also suggest only a modest apparent affinity decrease for the PMCA compared to those of the reduced counterparts (*10*). Consistent with these prior measurements, both CaM-L7 and CaM-$L7_{ox}$ form apparent high-affinity complexes with the C28W peptide (Figure 3). The complexes are in slow exchange on the NMR time scale, indicating tight binding, and the stoichiometry of each is 1:1. Dramatic improvements in the NMR spectra of CaM-L7 and CaM-$L7_{ox}$ are observed upon binding to C28W (Figure 3). Most of the conformational heterogeneity noted in the $^{1}H-^{15}N$ HSQC spectra of CaM-L7 and CaM-$L7_{ox}$ is alleviated by binding to C28W, as indicated by the reduced line widths and improved resolution in the $^{1}H-^{15}N$ HSQC spectra of these complexes. These results indicate that conformational heterogeneity introduced into CaM both by substitution of leucine for methionine and by oxidation of

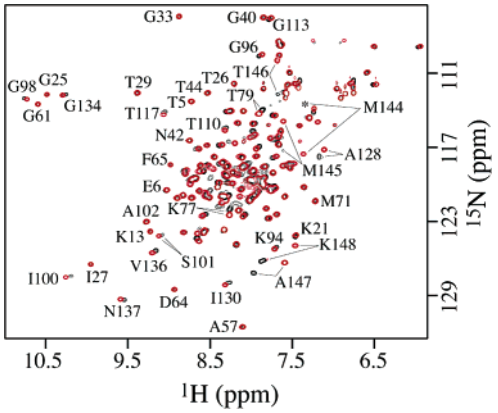

FIGURE 3: Effect of methionine oxidation on CaM-L7 structure in the CaM-L7−C28W complex. Two-dimensional ^{1}H−^{15}N HSQC spectra of CaM-L7 (red contours) and oxidized CaM-L7 (CaM-L7$_{ox}$, black contours), each bound to C28W, are shown. All of the main chain resonances of CaM-L7 and CaM-L7$_{ox}$ bound to C28W have been assigned. Some of the well-resolved resonances are indicated. Most of peaks corresponding to residues in the N-terminal domain experience little chemical shift perturbation when M144 and M145 are oxidized, whereas most of those in the C-terminal globular domain experience small to very large perturbations.

methionine is relieved to a large extent by binding to the C28W peptide.

Main Chain Chemical Shift Perturbations Indicate Large Structural Changes in the C-Terminal Domain when M144 and M145 Are Oxidized. Chemical shift changes are very sensitive indicators of local structural changes. The chemical shift changes for CaM-L7 in the complex with C28W resulting from oxidation of M144 and M145 provide the first comprehensive, site-resolved assessment of the structural changes underlying the nonproductive association between oxidized CaM and the PMCA. The main chain chemical shifts of the CaM portions of the complexes of ^{15}N- and ^{13}C-labeled CaM-L7 and ^{15}N- and ^{13}C-labeled CaM-L7$_{ox}$ with the C28W peptide were assigned using triple-resonance methods. The magnitudes of these shifts permit a comprehensive appraisal of the effect of oxidation of M144 and M145 (Figures 3 and 4). These data show that the main chain (and $^{13}C^{\beta}$) chemical shifts of residues in the N-terminal globular domain of CaM-L7 in the complex with C28W are affected little by oxidation of M144 and M145. The magnitudes of the changes for residues from the N-terminus through residue R74 (C-terminal end of helix D) are less than or equal to the noise associated with making the measurements (with the exception of V55; see the dashed line in the bottom panel of Figure 4). In contrast, significant changes are observed in the chemical shifts for most of the residues in the C-terminal globular domain and for some of the residues in the central linker region. The magnitudes of these changes are largest for the residues (F141, V142, Q143, M144, M145, T146, A147, and K148) nearest in sequence to the sites of oxidation, as might be expected. Thus, a significant perturbation of the C-terminal helix (helix H) is suggested. In addition, large main chain chemical shift changes (weighted average change of >0.1) are also observed for many other residues (I85, F89, F92, I100, L124, I125, A128, and Y138). Most of these latter residues contribute hydrophobic side chains to the hydrophobic pocket of the C-terminal globular domain or are in the proximity of the side chains of M144 and M145, and most contribute side

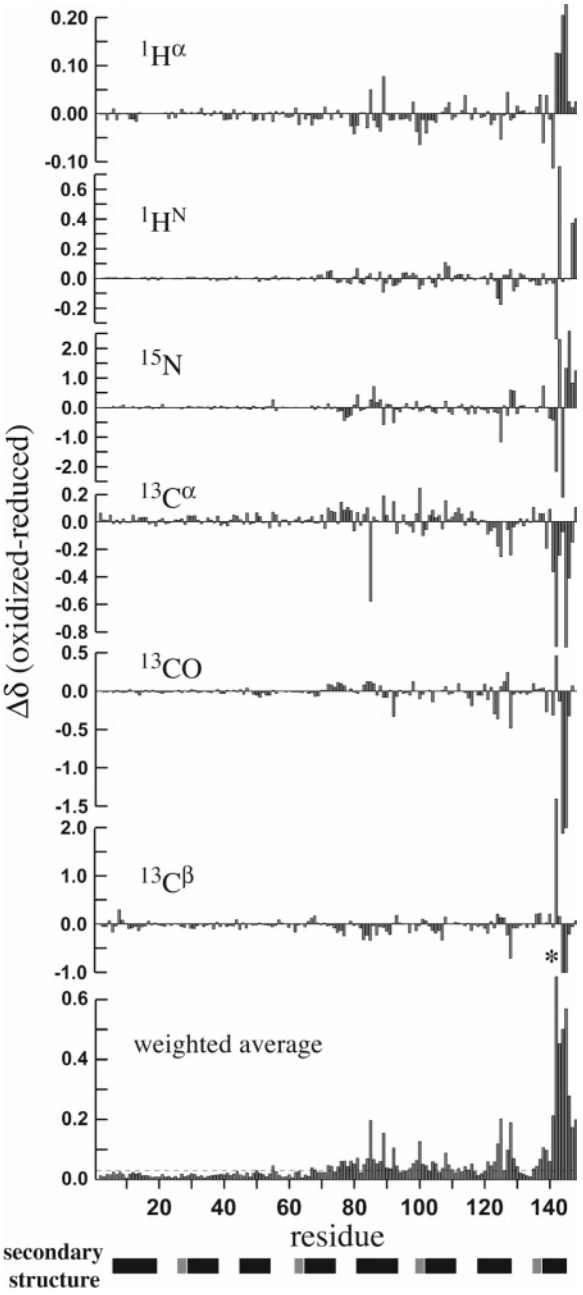

FIGURE 4: Main chain chemical shift changes in CaM-L7 in the CaM-L7−C28W complex upon methionine oxidation. The changes in the chemical shifts of the main chain and $^{13}C^{\beta}$ atoms for CaM-L7 in the CaM-L7−C28W complex that result from oxidation of M144 and M145 (oxidized minus reduced) are shown as a function of residue. The plot at the bottom shows an absolute value weighted average (*39*), calculated by normalizing the absolute value of each shift change by the absolute value of the largest change for that nucleus and then averaging for each position. The dashed line is drawn to indicate the approximate minimum significant change. The secondary structure is also shown (dark bars represent helices and light bars β-strands), determined using chemical shift index (CSI) analysis (*36*). The changes in the chemical shifts for the $^{13}C^{\beta}$ atoms of M144 and M145 are large (approximately −6 ppm) due to the proximity of this nucleus to the site of oxidation as discussed in the text, and are marked with an asterisk to indicate that these are truncated in the plot.

chains to the binding interface with target domains [for instance, the skeletal muscle myosin light chain kinase (*33*)], including the PMCA (*34*). The large changes in the main chain at residues 85, 89, and 92 (helix E) potentially communicate the effects of oxidation to the central linker

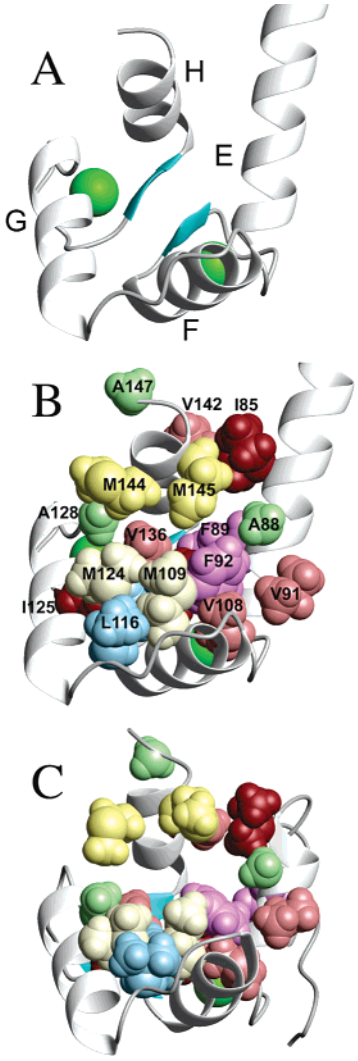

FIGURE 5: Spatial organization of amino acid side chains in the C-terminal domain of CaM. The main chain ribbon (A) of CaM (*41*) with secondary structure elements is shown for reference (β-strands colored cyan and Ca^{2+} represented by green spheres). The side chains of some of the amino acids experiencing large main chain and/or methyl group chemical shift perturbations in the CaM-$L7_{ox}$−C28W complex upon oxidation of M144 and M145 are rendered as space-filling (CPK) images with van der Waals radii on the CaM structure (B) (*41*) and on the solution structure of the complex of CaM with a short (C20W) peptide corresponding to the N-terminal portion of the CaM-binding domain of the PMCA (C) (*34*). Hydrogens were added to the CaM side chains using InsightII (Accelrys, Inc.). Side chains are colored by amino acid type: yellow/beige for Met, light green for Ala, brown for Ile, pink for Val, blue for Leu, and violet for Phe).

and to the N-terminal domain. The spatial organization of these side chains is summarized in Figure 5. Thus, the observed changes in the main chain chemical shifts upon oxidation of M144 and M145 indicate significant structural changes throughout the C-terminal globular domain that modify the binding pocket that recognizes target proteins. In addition, significant chemical shift changes are observed for residues considered to be the hinge residues of the central linker region, consistent with prior measurements indicating that the spatial arrangement of the opposing domains of CaM bound to C28W is altered upon methionine oxidation (*9*).

Unwinding of Helix H in CaM-L7 in the CaM-L7−C28W Complex upon Oxidation of M144 and M145. The assigned chemical shifts permit a detailed assessment of the secondary structure of the CaM-L7 portion of the CaM-L7−C28W complex (Figure 4) and the effects on the secondary structure of oxidation of M144 and M145 (*35*−*38*). Chemical shift index (CSI) analysis (*36*) using the $^1H^\alpha$, $^{13}C^\alpha$, ^{13}CO, and $^{13}C^\beta$ chemical shifts indicates that CaM-L7 bound to C28W contains eight helices (E6−F19, T29−S38, E45−E54, F65−R74, S81−N93, A102−N111, D118−A128, and Y138−M145) and four short β-strands (T26−T28, T62−D64, Y99−S101, and Q135−N137). This secondary structure is very typical of both wild-type CaM and CaM bound to target domains (*39*−*41*). Helix D (F65−R74) is somewhat shorter at its C-terminus than is normally assumed for wild-type CaM and is more consistent with that observed for CaM bound to targets (*39*), consistent with the CaM molecule bending via the central hinge region to accommodate interactions of C28W with both domains.

Upon oxidation of M144 and M145, the chemical shifts in the N-terminal domain of CaM-L7 in the CaM-L7−C28W complex change very little, whereas those in the central linker region and the C-terminal domain change substantially (Figure 4), as detailed above. The most dramatic changes occur for residues at the C-terminus (141−148), near in sequence to the sites of oxidation, and affect all of the main chain nuclei. Changes in the $^1H^\alpha$, $^{13}C^\alpha$, and ^{13}CO nuclei are good indicators of secondary structure change, and for the residues near the C-terminus and in the C-terminal helix (helix H), the increases in the $^1H^\alpha$ chemical shifts, the decreases in the $^{13}C^\alpha$ shifts, and the decreases in the ^{13}CO chemical shifts are all indicative of a change from α-helix to random coil (*36*, *38*). Whereas the CSI analysis indicates no change in secondary structure in the remainder of the molecule, a decrease in the length of the C-terminal helix is indicated upon oxidation of M144 and M145. Before oxidation, this helix includes residues Y138−M145. After oxidation, it is shortened by two residues (Y138−Q143). It is important to consider that oxidation of free methionine produces very large downfield changes in the ^1H and ^{13}C chemical shifts of nuclei adjacent to the sulfur (ϵ and γ positions) and large upfield changes in the chemical shifts of the nuclei at the β position, as evidenced by $^1H-^{13}C$ HSQC spectra of methionine and methionine sulfoxide produced by oxidation of methionine with H_2O_2 (not shown), but that positions more remote are relatively unaffected. The changes in the chemical shifts for the α nuclei are nominal when the sulfur is oxidized to the sulfoxide. The ^1HN, ^{15}N, ^{13}CO, $^{13}C^\alpha$, and $^1H^\alpha$ chemical shift changes noted for M144 and M145 (Figure 4) are, therefore, due to structural changes in the protein and not to oxidation of the methionine per se, and the ^{13}CO, $^{13}C^\alpha$, and $^1H^\alpha$ changes can be used in the CSI analysis. Thus, these results indicate that the C-terminal helix of CaM-L7 in the CaM-L7−C28W complex is shortened by two residues when M144 and M145 are oxidized, indicating a direct effect of oxidation on this particular secondary structural element. It is clear (Figure 5) that helix H and the M144 and M145 side chains play key structural roles in the C-terminal globular domain of CaM. Loss of helical structure for M144 and M145 most likely leads to the global structural changes in the C-terminal domain of CaM deduced from the main chain chemical shift changes.

Methyl Group Chemical Shift Perturbations Highlight Global Structural Changes in the CaM-L7−C28W Complex Accompanying M144 and M145 Oxidation. The methyl

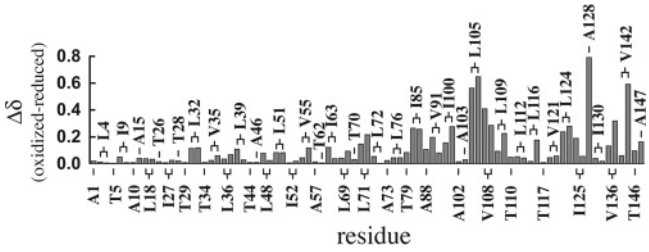

FIGURE 6: Methyl group chemical shift changes in CaM-L7 in the CaM-L7−C28W complex upon methionine oxidation. Weighted averages for the ^{1}H and ^{13}C chemical shift changes for the methyl groups in CaM-L7 in the CaM-L7−C28W complex resulting from oxidation of M144 and M145 are shown. The values were calculated as described in the legend of Figure 4. For Ile residues, the value for the γ_2 methyl group is located to the left, and that for the δ_1 position to the right. For Val (Leu) residues, the change for the γ_1 (δ_1) methyl group is located to the left and that for the γ_2 (δ_2) group to the right.

groups of amino acid side chains in CaM provide important intermolecular contacts with bound target domains and intramolecular contacts for maintenance of the tertiary structure of the individual globular CaM domains (*42*). In the complex of CaM-L7 with the C28W peptide, the perturbations of the chemical shifts of the methyl groups upon oxidation of M144 and M145 in CaM provide insight into changes in these contacts and the associated structural changes (Figure 6). In the C-terminal globular domain, oxidation of M144 and M145 produces substantial perturbations of the chemical shifts of many of the methyl groups. As with the perturbations of the main chain chemical shifts, these perturbations are large for methyl groups of residues near in sequence to the sites of oxidation (V142γ_2, for instance). Large changes (weighted average change of >0.1) are also noted for many of the methyl groups of residues that form the core of the hydrophobic pocket of the C-terminal globular domain (I85, A88, V91, I100, L105, V108, L109, L116, L124, I125, A128, V136, V142, and A147) and are commonly involved in interactions with target domains (*34*, *43*). Interestingly, some large changes are also observed for methyl groups of residues in the N-terminal domain (L32, L39, V55, I63, and L71) that commonly interact with target domains. The locations of the side chains bearing these methyl groups in the globular domains of CaM are shown in Figure 7. These data indicate clearly that a substantial reorganization of the tertiary structure of the C-terminal globular domain of CaM-L7 in the CaM-L7−C28W complex occurs when M144 and M145 are oxidized. These changes also lead to limited changes in the N-terminal domain, probably via the bound peptide. As noted above, the critical roles played by helix H and the side chains of M144 and M145 (Figure 5) suggest that the conformational switch leading to the global C-terminal domain changes is initiated by unwinding of helix H at M144 and M145 accompanying oxidation.

Diminished Intermolecular Contacts between CaM$_{ox}$ and C28W. The methyl group chemical shift perturbations suggest that the interactions between CaM-L7 and C28W in the CaM-L7−C28W complex are altered as a result of oxidation of M144 and M145 to the sulfoxides. Using isotope-filtered, edited NMR techniques (*27*), intermolecular NOEs between the uniformly isotopically labeled CaM-L7 portion of the complex and the unlabeled C28W portion can be selectively observed before and after oxidation of M144 and M145 to

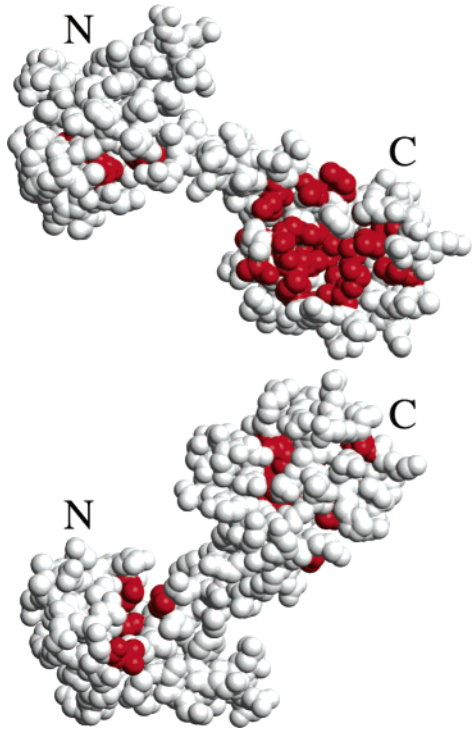

FIGURE 7: Localization of structural changes in CaM-L7 in the CaM-L7−C28W complex resulting from M144 and M145 oxidation as determined by methyl group chemical shift changes. Highlighted on the X-ray crystal structure of CaM (*41*) are side chains (red) of residues with methyl groups experiencing large chemical shift perturbations [weighted average of >0.1 (Figure 6)]. Two views are shown, one (top) exposing the hydrophobic pocket in the C-terminal domain and the other (bottom) the N-terminal pocket. Approximate van der Waals radii are rendered for the heavy atoms (no hydrogens are included). The figure was drawn with MOLMOL (*55*).

gauge the effects of oxidation (Figure 8). The results are quite dramatic. For M144 and M145 in CaM-L7, the ϵ-methyl groups are involved in many contacts with the peptide (many NOEs are observed between these methyl groups and protons on C28W), but when these methionine residues are oxidized, nearly all of these contacts are lost. Similar results are observed for other methyl groups in the C-terminal domain, particularly those experiencing very large chemical shift changes upon oxidation (for instance, V142, L124, and L105; see Figure 8). Other, somewhat less dramatic results are also noted (for instance, I100). In the N-terminal globular domain, the contacts observed between some of the important methyl groups involved in interactions with the C28W peptide are not dramatically altered upon oxidation of M144 and M145. For V55, L39, and L32, for instance (Figure 8), there are small changes observed in the intermolecular NOEs to the methyl groups of the side chains of these amino acids, but they are quite limited compared to the changes noted in the C-terminal domain. These data show that the tertiary structural changes in the C-terminal globular domain of CaM-L7 originating from oxidation of M144 and M145 lead to extensive changes in the intermolecular interface with the target C28W peptide. The changes in the contacts between C28W and the N-terminal domain are small and, like the chemical shift changes, reflect less dramatic changes in the N-terminal domain. These could simply be mediated by the C28W peptide as a result of altered interactions with the C-terminal globular domain, or they

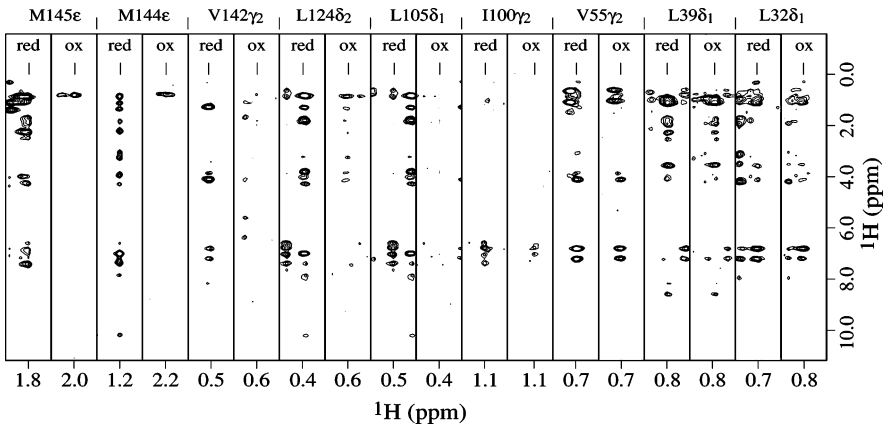

FIGURE 8: Oxidation of M144 and M145 alters intermolecular contacts between CaM-L7 and C28W. Two-dimensional strips from a three-dimensional ^{13}C F_1-filtered, F_3-edited NOESY-HSQC experiment (*27*) are shown for several methyl groups in CaM-L7 involved in intermolecular contacts with C28W. The NOEs between these methyl groups and protons on the C28W peptide are shown in the strips. The changes in these contacts (NOEs) upon oxidation of M144 and M145 in the complex are also shown (red for reduced and ox for oxidized).

could reflect an altered structural coupling between the N- and C-terminal globular domain mediated by the central linker region (*4*), or perhaps a combination of both.

DISCUSSION

CaM Activation of the PMCA. The autoinhibitory domain of the plasma membrane Ca^{2+}-ATPase (PMCA) is located at the C-terminus and includes the 28-amino acid CaM-binding sequence (*44*−*48*). Fluorescence lifetime measurements of CaM (Ca^{2+}_4-CaM) bound to the PMCA indicate a rotational correlation time consistent with CaM bound to a domain that is physically dissociated from the rest of the protein (*49*). Dissociation of this domain activates the PMCA. More recently, these suggestions have been supported by the results of single-molecule polarization modulation experiments (*11*). Under conditions where the Ca^{2+} binding sites of CaM are all occupied (saturating Ca^{2+} concentration), the observed modulation depth distribution reveals a single population with a low average depth indicating high mobility, suggesting that CaM binds to the autoinhibitory domain and dissociates this domain from the rest of the PMCA. The increased mobility of the dissociated domain results in a shorter rotational correlation time and the observed decreased modulation depth. This dissociation presumably restores access of substrates (Ca^{2+} and ATP) to the active site, thus activating the PMCA.

CaM_{ox} Activation of the PMCA. Oxidized CaM (CaM_{ox}) binds to the PMCA but is not able to fully activate it (*3*−*5*, *9*−*12*) specifically because of oxidation of M144 and M145 (*3*, *9*, *10*). The degree of activation (*10*) correlates with the ratio of mobile and immobile populations observed in single-molecule polarization experiments (*11*). In these experiments using CaM_{ox}, two populations are observed: one similar to that observed with Ca^{2+}_4-CaM and a second with a higher average modulation depth and broader distribution, evidently arising from a species with CaM_{ox} bound to the autoinhibitory domain without triggering dissociation (large modulation depth, large rotational correlation time, and low mobility). Given the premise that binding of CaM to the PMCA induces the proper structural changes in the autoinhibitory domain to promote dissociation of this domain and thus PMCA activation, these results suggest that CaM_{ox} is only capable of promoting these changes some of the time.

Oxidation-Induced Structural Changes in CaM. The inability of CaM_{ox} to induce the requisite structural changes in the autoinhibitory domain of the PMCA necessary for PMCA activation originates in the changes in CaM structure caused by M144 and M145 oxidation. Our results provide the first site-resolved description of the structural changes in CaM accompanying M144 and M145 oxidation that are responsible for the nonproductive interaction with the PMCA. First, the circular dichroism results indicate that secondary structural changes associated with oxidation of M144 and M145 are limited, and in the context of the CaM-L7−C28W complex are localized to the C-terminal helix (helix H) of CaM. The chemical shift changes indicate a general trend in this helix toward random coil and away from α-helical character, whereas an analysis based on the chemical shift index indicates a definitive shortening of this helix by two residues. Helix H plays many important roles in CaM (Figure 5): assisting to maintain the proper spacing between secondary structural elements in the C-terminal globular domain and their relative orientations, communicating information to the central helix region and perhaps the N-terminal domain via contacts with helix E, and participating in recognition of target domains. The models in Figure 5 would suggest that helical character at M144 and M145 in helix H is important for proper positioning of M144 and M145 side chains and that random coil character would significantly perturb both structure and recognition.

Both the main chain and side chain chemical shift changes of the amino acids in CaM-L7 in the CaM-L7−C28W complex indicate clearly that large tertiary structural changes in the C-terminal globular domain accompany oxidation of M144 and M145. These include residues in the calcium binding loops, resulting in the observed decreases in calcium affinity associated with methionine oxidation (*3*, *13*). Because the secondary structure changes are nominal, the results suggest a global tertiary structural reorganization of the C-terminal domain. Significant changes are also indicated for the central linker region, whereas smaller changes are noted for the N-terminal domain. The changes in the N-terminal domain and central linker region could be mediated by the peptide as a result of the altered interactions with the C-terminal domain, or their origins could stem from an altered disposition of the two domains mediated by the

central linker region also resulting from the C-terminal domain reorganization (*4*). Dramatic changes in the intermolecular interface between CaM-L7 and C28W also arise when M144 and M145 are oxidized. The contacts between C28W and the methyl groups of M144 and M145 are lost, as are many of those between C28W and other methyl groups in the C-terminal globular domain that comprise the interface.

CaM−C28W Complex. The conformational heterogeneity observed in NMR spectra of CaM-L7 resulting from the substitution of leucine residues for methionine is dramatically eliminated when CaM-L7 binds to the C28W peptide. The secondary structure of CaM-L7 bound to C28W shows that helix D is shortened at its C-terminus, consistent with the CaM molecule bending at the central hinge region and interacting via both of the opposing globular domains with the target domain. The isotope-filtered, isotope-edited NMR experiments clearly identify side chains in both the N- and C-terminal domains of CaM-L7 that contact the C28W in the complex. These data point to a structure for the CaM-L7−C28W complex that, in many ways, is similar to some of the classic complexes of CaM with target domains (*42*). It should be noted that the methyl group-containing side chains in the C-terminal globular domain that interact with the C28W peptide include those shown to interact with the C20W peptide (C28W lacking the eight C-terminal residues) in the CaM−C20W complex (*34*), and thus, these complexes are similar in this respect. The C20W peptide does not contact the N-terminal domain of CaM in the CaM−C20W complex, and the CaM−C20W complex is unusual in this respect. Although either the isolated C-terminal (*50*, *51*) or N-terminal (*50*) domain of CaM can serve to activate the PMCA, both the N-terminal and C-terminal sites on the CaM binding sequence of the PMCA must be occupied for PMCA activation (*50*). Thus, given our results and the functional results (*10*), all indications are that the CaM-L7−C28W complex, and the structural changes in the complex that occur upon oxidation, accurately reproduce the situation with the full-length wild-type proteins.

Mechanism of Methionine Oxidation-Induced Loss of Function. Neither M144 nor M145 in CaM is essential for activation of the PMCA. Substitution of both of these methionine residues with glutamine results in a CaM molecule that is able to fully activate the PMCA (*52*), although the apparent dissociation constant for the complex is increased somewhat. Although glutamine is not as strong a helix former as methionine (*53*, *54*), glutamine would be expected to maintain the helical character of the C-terminal helix. The precise structural consequences of these glutamine substitutions are not known, but fluorescence measurements indicate that they do not substantially affect the structure of the carboxy-terminal globular domain of CaM (*52*). Clearly, the overall increase in polarity due to these substitutions and the lack of contacts to the methyl groups of the missing methionine side chains do not result in loss of function with respect to fully activating the PMCA. A CaM mutant lacking residues M145−K148 is also able to fully activate the PMCA, demonstrating again that M145 is not essential for this activation.

These previous results suggest that the inability of CaM with M144 and M145 oxidized to fully activate the PMCA is not the result of the inability of the methionine sulfoxides to form the appropriate contacts, per se. Nor is it simply an issue of polarity (*28*). Rather, methionine sulfoxide at M144 and M145 prevents the C-terminal globular domain from adopting the tertiary structure essential for PMCA activation. Because the secondary structure of the C-terminal helix of CaM is compromised by M144 and M145 oxidation, the suggestion is that, relative to that of methionine, the helical propensity of methionine sulfoxide is low, and the sulfoxides at M144 and M145 destabilize the helix. Furthermore, the presence of random coil character at positions 144 and 145 combined with the polarity change is a significant structural perturbant that promotes a global reorganization of the tertiary structure of the C-terminal domain as well as changes in the central linker region. This altered conformation is not able to activate the PMCA. In contrast, as noted above, removing part of the C-terminal helix is not perturbing, and replacing M144 and M145 with Gln still allows the C-terminal helix to form, which permit maintenance of the proper tertiary structure in the C-terminal domain as a whole. Thus, the ability of CaM_{ox} to partially activate the PMCA would then reflect the inherent equilibrium between CaM_{ox} with residues 144 and 145 in the helical versus random coil configuration when bound to the PMCA. Likewise, the population ratio of the observed species in the single-molecule experiments would correspond to CaM_{ox}−PMCA complexes with the C-terminal helix of CaM_{ox} intact (active, autoinhibitory domain dissociated) or compromised (inactive, autoinhibitory domain not dissociated). It is also important to consider that the different isomers of methionine sulfoxide might have measurably different helix propensities, and the extent of PMCA activation might reflect this isomeric dependence and the isomeric ratio.

Conclusions. Oxidation of the carboxyl-terminal methionine residues in CaM to the sulfoxides mediates PMCA recognition and activation. Oxidation promotes the switch to a conformation unable to activate the PMCA, characterized by a destabilized, shortened C-terminal helix, and a restructured C-terminal globular domain and central linker region. A loss of important contacts at the interface of CaM in this conformation and the PMCA inevitably prevents stabilization of the CaM-binding sequence of the enzyme and hence enzyme activation. Avenues for further investigation include high-resolution characterization of the structure of oxidized CaM and the CaM binding domain of the PMCA bound to oxidized CaM, studies of the physical basis for the methionine sulfoxide-induced switch, including measurements of the helix propensity of methionine sulfoxide, and determination of the relative efficacies of the isomers of methionine sulfoxide at the C-terminal positions in promoting the conformational switch.

ACKNOWLEDGMENT

We thank Carey Johnson, Krzysztof Kuczera, Asma Zaidi, and the members of the Johnson research group for insightful discussions and for sharing their related research results. We thank Todd Williams for mass spectrometry expertise and for performing the mass spectrometry. We thank Lewis Kay for Varian NMR pulse sequences.

REFERENCES

1. Yap, K. L., Kim, J., Truong, K., Sherman, M., Yuan, T., and Ikura, M. (2000) Calmodulin target database, *J. Struct. Funct. Genomics 1*, 8−14.

2. O'Neil, K. T., and DeGrado, W. F. (1990) How calmodulin binds its targets: Sequence independent recognition of amphiphilic α-helices, *Trends Biochem. Sci. 15*, 59−64.
3. Yao, Y., Yin, D., Jas, G. S., Kuczera, K., Williams, T. D., Schoneich, C., and Squier, T. C. (1996) Oxidative modification of a carboxyl-terminal vicinal methionine in calmodulin by hydrogen peroxide inhibits calmodulin-dependent activation of the plasma membrane Ca-ATPase, *Biochemistry 35*, 2767−2787.
4. Gao, J., Yin, D. H., Yao, Y., Sun, H., Qin, Z., Schoneich, C., Williams, T. D., and Squier, T. C. (1998) Loss of conformational stability in calmodulin upon methionine oxidation, *Biophys. J. 74*, 1115−1134.
5. Yin, D., Kuczera, K., and Squier, T. C. (2000) The sensitivity of carboxyl-terminal methionines in calmodulin isoforms to oxidation by H_2O_2 modulates the ability to activate the plasma membrane Ca-ATPase, *Chem. Res. Toxicol. 13*, 103−110.
6. Guerini, D., Krebs, J., and Carafoli, E. (1987) Stimulation of the erythrocyte Ca^{2+}-ATPase and of bovine brain cyclic nucleotide phosphodiesterase by chemically modified calmodulin, *Eur. J. Biochem. 170*, 35−42.
7. Wolff, J., Cook, G. H., Goldhammer, A. R., and Berkowitz, S. A. (1980) Calmodulin activates prokaryotic adenylate cyclase, *Proc. Natl. Acad. Sci. U.S.A. 77*, 3841−3844.
8. Walsh, M., and Stevens, F. C. (1977) Chemical modification studies on the Ca^{2+}-dependent protein modulator of cyclic nucleotide phosphodiesterase, *Biochemistry 16*, 2742−2749.
9. Gao, J., Yao, Y., and Squier, T. C. (2001) Oxidatively modified calmodulin binds to the plasma membrane Ca-ATPase in a nonproductive and conformationally disordered complex, *Biophys. J. 80*, 1791−1801.
10. Bartlett, R. K., Bieber Urbauer, R. J., Anbanandam, A., Smallwood, H. S., Urbauer, J. L., and Squier, T. C. (2003) Oxidation of Met144 and Met145 in calmodulin blocks calmodulin dependent activation of the plasma membrane Ca-ATPase, *Biochemistry 42*, 3231−3238.
11. Osborn, K. D., Bartlett, R. K., Mandal, A., Zaidi, A., Urbauer, R. J., Urbauer, J. L., Galeva, N., Williams, T. D., and Johnson, C. K. (2004) Single-molecule dynamics reveal an altered conformation for the autoinhibitory domain of plasma membrane Ca^{2+}-ATPase bound to oxidatively modified calmodulin, *Biochemistry 43*, 12937−12944.
12. Gao, J., Yin, D., Yao, Y., Williams, T. D., and Squier, T. C. (1998) Progressive decline in the ability of calmodulin isolated from aged brain to activate the plasma membrane Ca-ATPase, *Biochemistry 37*, 9536−9548.
13. Lafitte, D., Tsvetkov, P. O., Devred, F., Toci, R., Barras, F., Briand, C., Makarov, A. A., and Haiech, J. (2002) Cation binding mode of fully oxidised calmodulin explained by the unfolding of the apostate, *Biochim. Biophys. Acta 1600*, 105−110.
14. Strasburg, G. M., Hogan, M., Birmachu, W., Thomas, D. D., and Louis, C. F. (1988) Site-specific derivatives of wheat germ calmodulin. Interactions with troponin and sarcoplasmic reticulum, *J. Biol. Chem. 263*, 542−548.
15. Klee, C. B., and Vanaman, T. C. (1982) Calmodulin, *Adv. Protein Chem. 35*, 213−321.
16. Whitmore, L., and Wallace, B. A. (2004) DICHROWEB, an online server for protein secondary structure analyses from circular dichroism spectroscopic data, *Nucleic Acids Res. 32*, W668−W673.
17. Lobley, A., Whitmore, L., and Wallace, B. A. (2002) DICHROWEB: An interactive website for the analysis of protein secondary structure from circular dichroism spectra, *Bioinformatics 18*, 211−212.
18. Lobley, A., and Wallace, B. A. (2001) Dichroweb: A website for the analysis of protein secondary structure from circular dichroism spectra, *Biophys. J. 80*, 373a.
19. Sreerama, N., and Woody, R. W. (2000) Estimation of protein secondary structure from circular dichroism spectra: Comparison of CONTIN, SELCON, and CDSSTR methods with an expanded reference set, *Anal. Biochem. 287*, 252−260.
20. Sreerama, N., Venyaminov, S. Y., and Woody, R. W. (2000) Estimation of protein secondary structure from circular dichroism spectra: Inclusion of denatured proteins with native proteins in the analysis, *Anal. Biochem. 287*, 243−251.
21. Compton, L. A., and Johnson, W. C., Jr. (1986) Analysis of protein circular dichroism spectra for secondary structure using a simple matrix multiplication, *Anal. Biochem. 155*, 155−167.
22. Manavalan, P., and Johnson, W. C., Jr. (1987) Variable selection method improves the prediction of protein secondary structure from circular dichroism spectra, *Anal. Biochem. 167*, 76−85.
23. Wishart, D. S., Bigam, C. G., Yao, J., Abildgaard, F., Dyson, H. J., Oldfield, E., Markley, J. L., and Sykes, B. D. (1995) ^1H, ^{13}C and ^{15}N chemical shift referencing in biomolecular NMR, *J. Biomol. NMR 6*, 135−140.
24. Yamazaki, T., Forman-Kay, J. D., and Kay, L. E. (1993) Two-Dimensional NMR Experiments for Correlating ^{13}C-β and ^1H-δ/ϵ Chemical Shifts of Aromatic Residues in ^{13}C-Labeled Proteins via Scalar Couplings, *J. Am. Chem. Soc. 115*, 11054−11055.
25. Zerbe, O., Szyperski, T., Ottiger, M., and Wuthrich, K. (1996) Three-dimensional ^1H-TOCSY-relayed ct-[^{13}C,^1H]-HMQC for aromatic spin system identification in uniformly ^{13}C-labeled proteins, *J. Biomol. NMR 7*, 99−106.
26. Neri, D., Szyperski, T., Otting, G., Senn, H., and Wuthrich, K. (1989) Stereospecific nuclear magnetic resonance assignments of the methyl groups of valine and leucine in the DNA-binding domain of the 434 repressor by biosynthetically directed fractional ^{13}C labeling, *Biochemistry 28*, 7510−7516.
27. Zwahlen, C., Legault, P., Vincent, S. J. F., Greenblatt, J., Konrat, R., and Kay, L. E. (1997) Methods for measurement of intermolecular NOEs by multinuclear NMR spectroscopy: Application to a bacteriophage λ N-peptide/*boxB* RNA complex, *J. Am. Chem. Soc. 119*, 6711−6721.
28. Vogt, W. (1995) Oxidation of methionyl residues in proteins: Tools, targets, and reversal, *Free Radical Biol. Med. 18*, 93−105.
29. Sharov, V. S., Ferrington, D. A., Squier, T. C., and Schoneich, C. (1999) Diastereoselective reduction of protein-bound methionine sulfoxide by methionine sulfoxide reductase, *FEBS Lett. 455*, 247−250.
30. Sharov, V. S., and Schoneich, C. (2000) Diastereoselective protein methionine oxidation by reactive oxygen species and diastereoselective repair by methionine sulfoxide reductase, *Free Radical Biol. Med. 29*, 986−994.
31. Sun, H., Gao, J., Ferrington, D. A., Biesiada, H., Williams, T. D., and Squier, T. C. (1999) Repair of oxidized calmodulin by methionine sulfoxide reductase restores ability to activate the plasma membrane Ca-ATPase, *Biochemistry 38*, 105−112.
32. Ferrington, D. A., Sun, H., Murray, K. K., Costa, J., Williams, T. D., Bigelow, D. J., and Squier, T. C. (2001) Selective degradation of oxidized calmodulin by the 20S proteasome, *J. Biol. Chem. 276*, 937−943.
33. Ikura, M., Kay, L. E., Barbato, G., Spera, S., and Bax, A. (1992) Multidimensional NMR: Studies on Calmodulin and Its Complex with a Skeletal-Muscle Myosin Light-Chain Kinase Fragment, *FASEB J. 6*, A403.
34. Elshorst, B., Hennig, M., Forsterling, H., Diener, A., Maurer, M., Schulte, P., Schwalbe, H., Griesinger, C., Krebs, J., Schmid, H., Vorherr, T., and Carafoli, E. (1999) NMR solution structure of a complex of calmodulin with a binding peptide of the Ca^{2+} pump, *Biochemistry 38*, 12320−12332.
35. Wishart, D. S., Sykes, B. D., and Richards, F. M. (1992) The Chemical-Shift Index: A Fast and Simple Method for the Assignment of Protein Secondary Structure through NMR Spectroscopy, *Biochemistry 31*, 1647−1651.
36. Wishart, D. S., and Sykes, B. D. (1994) The ^{13}C Chemical-Shift Index: A Simple Method for the Identification of Protein Secondary Structure Using ^{13}C Chemical-Shift Data, *J. Biomol. NMR 4*, 171−180.
37. Wishart, D. S., Sykes, B. D., and Richards, F. M. (1991) Relationship between Nuclear Magnetic Resonance Chemical Shift and Protein Secondary Structure, *J. Mol. Biol. 222*, 311−333.
38. Spera, S., and Bax, A. (1991) Empirical Correlation between Protein Backbone Conformation and Cα and Cβ ^{13}C Nuclear Magnetic Resonance Chemical Shifts, *J. Am. Chem. Soc. 113*, 5490−5492.
39. Ikura, M., Kay, L. E., Krinks, M., and Bax, A. (1991) Triple-Resonance Multidimensional NMR Study of Calmodulin Complexed with the Binding Domain of Skeletal Muscle Myosin Light-Chain Kinase: Indication of a Conformational Change in the Central Helix, *Biochemistry 30*, 5498−5504.
40. Ikura, M., Spera, S., Barbato, G., Kay, L. E., Krinks, M., and Bax, A. (1991) Secondary Structure and Side-Chain ^1H and ^{13}C Resonance Assignments of Calmodulin in Solution by Heteronuclear Multidimensional NMR Spectroscopy, *Biochemistry 30*, 9216−9228.

41. Babu, Y. S., Bugg, C. E., and Cook, W. J. (1988) Structure of calmodulin refined at 2.2 Å resolution, *J. Mol. Biol. 204*, 191−204.
42. Crivici, A., and Ikura, M. (1995) Molecular and structural basis of target recognition by calmodulin, *Annu. Rev. Biophys. Biomol. Struct. 24*, 85−116.
43. Ikura, M., Clore, G. M., Gronenborn, A. M., Zhu, G., Klee, C. B., and Bax, A. (1992) Solution Structure of a Calmodulin-Target Peptide Complex by Multidimensional NMR, *Science 256*, 632−638.
44. Padanyi, R., Paszty, K., Penheiter, A. R., Filoteo, A. G., Penniston, J. T., and Enyedi, A. (2003) Intramolecular interactions of the regulatory region with the catalytic core in the plasma membrane calcium pump, *J. Biol. Chem. 278*, 35798−35804.
45. Verma, A. K., Enyedi, A., Filoteo, A. G., and Penniston, J. T. (1994) Regulatory region of plasma membrane Ca^{2+} pump. 28 residues suffice to bind calmodulin but more are needed for full auto-inhibition of the activity, *J. Biol. Chem. 269*, 1687−1691.
46. James, P., Maeda, M., Fischer, R., Verma, A. K., Krebs, J., Penniston, J. T., and Carafoli, E. (1988) Identification and primary structure of a calmodulin binding domain of the Ca^{2+} pump of human erythrocytes, *J. Biol. Chem. 263*, 2905−2910.
47. Falchetto, R., Vorherr, T., Brunner, J., and Carafoli, E. (1991) The plasma membrane Ca^{2+} pump contains a site that interacts with its calmodulin-binding domain, *J. Biol. Chem. 266*, 2930−2936.
48. Falchetto, R., Vorherr, T., and Carafoli, E. (1992) The calmodulin-binding site of the plasma membrane Ca^{2+} pump interacts with the transduction domain of the enzyme, *Protein Sci. 1*, 1613−1621.
49. Yao, Y., Gao, J., and Squier, T. C. (1996) Dynamic structure of the calmodulin-binding domain of the plasma membrane Ca-ATPase in native erythrocyte ghost membranes, *Biochemistry 35*, 12015−12028.
50. Sun, H., and Squier, T. C. (2000) Ordered and cooperative binding of opposing globular domains of calmodulin to the plasma membrane Ca-ATPase, *J. Biol. Chem. 275*, 1731−1738.
51. Guerini, D., Krebs, J., and Carafoli, E. (1984) Stimulation of the purified erythrocyte Ca^{2+}-ATPase by tryptic fragments of calmodulin, *J. Biol. Chem. 259*, 15172−15177.
52. Yin, D., Sun, H., Weaver, R. F., and Squier, T. C. (1999) Nonessential role for methionines in the productive association between calmodulin and the plasma membrane Ca-ATPase, *Biochemistry 38*, 13654−13660.
53. Chou, P. Y., and Fasman, G. D. (1978) Prediction of the secondary structure of proteins from their amino acid sequence, *Adv. Enzymol. Relat. Areas Mol. Biol. 47*, 45−148.
54. Chou, P. Y., and Fasman, G. D. (1978) Empirical predictions of protein conformation, *Annu. Rev. Biochem. 47*, 251−276.
55. Koradi, R., Billeter, M., and Wuthrich, K. (1996) MOLMOL: A program for display and analysis of macromolecular structures, *J. Mol. Graphics 14*, 51−55.

BI0504963